Journal of Chromatography, 544 (1991) 413–443
Elsevier Science Publishers B.V., Amsterdam

CHROM. 23 038

Review

Design requirements of silica-based matrices for biopolymer chromatography

M. P. HENRY
Research and Development Laboratories, J. T. Baker Inc., Phillipsburg, NJ (U.S.A.)

ABSTRACT

This work briefly reviews the philosophy which has guided the design of bonded phases for biopolymer chromatography in our laboratories, since 1980. Its main purpose, however, is to examine closely the physical and chemical nature of these bonded phases, which determine, in part, their chromatographic properties. Thus several physical properties and characterization methods of the substrate, porous silica, were described. Aspects of the design and synthesis of wide-pore bonded phases have been illustrated, in which trifunctional silanes were reacted covalently with the substrate under polymer-forming conditions in all cases. Finally a three-tier characterization approach has been applied, in which physical, chemical and chromatographic properties of the bonded phase are measured. The objectives of characterization have been to determine (1) the nature of the bonded phase surface, (2) its influence on chromatographic performance, and (3) the influence of various synthetic processes upon bonded phase reproducibility.

CONTENTS

1. Introduction 414
2. Materials, methods and results 416
   2.1. Materials 416
   2.2. Methods 416
      2.2.1. Column "titration" method 417
   2.3. Results 418
3. Discussion 418
   3.1. Physical properties and characterization of porous silica 420
      3.1.1. Particle size distribution 420
      3.1.2. Pore size and pore size distribution 422
      3.1.3. Pore volumes and surface areas 427
      3.1.4. Reproducibility of silicas 427
   3.2. Bonded phase design and synthesis 428
   3.3. Characterization of bonded phases 429
      3.3.1. Physical methods 429
      3.3.2. Chemical methods 430
      3.3.3. Chromatographic methods 436

0021-9673/91/$03.50

4. Appendix 1: Definition of terms 441
5. Appendix 2: Derivation of equations 441
6. Acknowledgements 442
References 443

1. INTRODUCTION

Over the past decade, research in our laboratories has led to the development and commercialization of silica-based *matrices* for biochromatography [1]. Specifically we have designed reversed phases, ion exchangers and hydrophobic interactors suitable for peptides, proteins, oligonucleotides and oligosaccharides. The commercially available matrices are listed in Table 1.

TABLE 1

COMMERCIALLY AVAILABLE BAKERBOND WIDE-PORE BONDED PHASES FOR BIOPOLYMER CHROMATOGRAPHY

Nominal pore diameters are 30 nm. BakerBond, BakerBond Wide-Pore, BakerBond ABx, QUAT, Carboxy-sulfon, HI-Propyl are trademarks of J. T. Baker Inc.

Name[a]	Mechanism	Particle size (μm)
BakerBond Wide-Pore Octadecyl	Reversed phase	5, 15, 22, 40
BakerBond Wide-Pore Octyl	Reversed phase	5, 15
BakerBond Wide-Pore Butyl	Reversed phase	5, 15, 40
BakerBond Wide-Pore PEI	Weak anion exchange	5, 15, 40
BakerBond Wide-Pore CBX	Weak cation exchange	5, 15, 40
BakerBond Wide-Pore HI-Propyl	Hydrophobic interaction	5, 14, 40
BakerBond Wide-Pore ABx	Mixed cation/anion exchange	5, 15, 40
BakerBond Wide-Pore CSX	Strong cation exchange	5, 15, 40
BakerBond Wide-Pore QUAT	Strong anion exchange	5, 15, 40

[a] PEI = Polyethyleneimine; CBx = carboxyethyl; CSX = Carboxy-sulfon (trademark of J. T. Baker); QUAT = quaternary ammonium, functional groups.

The successful design of these packings rests upon a clear perception of those properties that are necessary and desirable for the practice of biochromatography. These properties are listed in Table 2.

With these requirements in mind, porous silica was selected as the substrate because of its many well-recognized advantages and few limitations.

Porous silica is amenable to a range of characterization methods to ensure reproducibility [1]. Specifications, which are developed from these properties, are crucial in the overall design of bonded phases. Some of the properties which are routinely measured in our laboratories are listed in Table 3.

The bonding chemistry we chose can be broadly classified as that which results in a polymer layer covalently bound to a silica surface. This layer will have properties such as thickness, volume and density; and will alter the pore diameter, pore volume and surface area of those silicas which it covers.

All bonded phases are prepared using trifunctional silanes of the general formula:

$$R\text{–}SiX_3 \qquad (1)$$

TABLE 2

DESIRABLE PROPERTIES OF PACKINGS FOR BIOPOLYMER CHROMATOGRAPHY

Property	Physico-chemical implications
High resolution, speed	Small particles, large pores (30 nm), rigid
High recoveries (mass and activity)	Lack of non-specific binding, non-denaturing surface
High capacity	High surface area, large pores
High stability	Low tendency to hydrolysis
Convenience of use	High flow-rates, incompressible, stored dry
Universality of methodology	Same packing substrate and surface characteristics regardless of particle size
Versatility	Substrate available in wide range of particle and pore diameters, surface areas and pore volumes. Compatible with wide range of buffers, salts and chaotropic agents
Regenerability	Range of cleaning solvents available
Sterilizability	Organic solvent compatible; acid and base stable
Microbial inertness	Synthetic substrate
Reproducibility	Control over surface chemistry and properties of substrate such as surface area, pore diameter, pore volume and surface activity

where R can be a wide range of functional groups including polymers, and X can be a methoxy, ethoxy or halogen. Non-polar phases for reversed-phase chromatography are synthesized under polymer-forming conditions. Polar phases for ion-exchange and hydrophobic interaction chromatography are prepared in a two- or three-stage reaction wherein a hydrophilic, reactive polymer is covalently bound to the silica surface and subsequently reacted to incorporate, in a second layer, charged and weakly non-polar groups. The choices of substrate and bonding chemistry result in a family of bonded phases which meet almost all the requirements listed in Table 2.

A series of characterization methods needs to be devised, to ensure both the reproducibility of manufacture and the meeting of performance standards. These methods can be classified as physical, chemical and chromatographic. Characterization methods and data arising from their application are rarely published by

TABLE 3

PROPERTIES OF SILICA USED TO DETERMINE REPRODUCIBILITY AND SET SPECIFICATIONS

Appearance
%C, %H
pH of 5% suspension in 0.1 *M* KCl
Loss on drying
Iron
Particle size distribution
Mean pore diameter
Specific surface area
Pore volume
Octadecyl bonding test (C, H ligand density; selectivity of packed column)

manufacturers; even though much of this information can aid the chromatographer in the selection and use of the chromatographic materials. Furthermore, an understanding of the physico-chemical character of the bonded phase surface, contributes to the determination of separation mechanisms and selectivity prediction.

It is the aim of this review, therefore, to describe the characteristics of the silicas we chose, and the preparation, physico-chemical properties and characterization of the bonded phases synthesized from this substrate.

2. MATERIALS, METHODS AND RESULTS

2.1. Materials

All silicas, bonded phases, packed columns and chemicals were obtained from J. T. Baker. Proteins were purchased from Sigma. Standard solutions of phenanthro [3,4-*c*]phenanthrene, tetrabenzonaphthalene and benzo[*a*]pyrene, were generously donated by Dr. Lane C. Sander, National Institute of Standards and Technology.

2.2. Methods

Mercury porosimetry was carried out using standard methods [3,4]. All values of pore diameters, surface areas and pore volumes in this review were obtained by this technique except where indicated. Values of pore diameters given here are median values. In other words the mid-point of the population. Analyses of C, H and N levels in bonded phases, were obtained by standard methods in our laboratories. Tests listed in Table 4 are performed using procedures developed at J.T. Baker.

The colorimetric methods used to calculate carboxyl group content is described elsewhere [5].

Protein capacities were determined by pumping their solutions through packed columns until absorbance of the breakthrough reached 50% of that of the original

TABLE 4

BONDED PHASE AND BONDED LAYER PHYSICAL PROPERTIES TO CHARACTERIZE MATRICES FOR BIOPOLYMER CHROMATOGRAPHY

Property	Symbol	Definition	Units
Ligand density	Lig. D	Moles of a given functional group/unit area of surface	μmol/m^2
Layer thickness	LT	Thickness of bonded layer	nm
Specific layer volume	SLV	Volume of bonded layer/unit area of surface	mm^3/m^2
Layer density	LD	Weight of layer divided by its volume	g/ml
Pore diameter	PD_s or PD_p	Median pore diameter (substrate or phase)	nm
Pore volume	PV_s or PV_p	Volume within pores (substrate or phases)	ml/g
Surface area	SA_s or SA_p	Total specific area of all pores (substrate or phase)	m^2/g
%Organic		% By weight of bonded phase that is organic	None

TABLE 5

METHODS FOR CALCULATION OF BONDED PHASE AND BONDED LAYER PROPERTIES DEFINED IN TABLE 4

Property	Equation		Units
Ligand density	$10^3 \cdot \%C/1.2 \cdot SA = Lig.\ D$	(2)	μmol of C per m^2
	$10^3 \cdot \%C/1.2 \cdot$ carbon atoms per ligand chain $\cdot SA$	(3)	μmol of ligand per m^2
Specific layer volume	$SLV = (PV_s - PV_p)10^3/SA_s$	(4)	mm^3/m^2
Layer density	$\frac{\%Organic}{100} \cdot \frac{1}{PV_s - PV_p} = LD$	(5)	g/ml
Layer thickness	$LT_1 = SLV$, expressed in nm	(6)	nm
	or $LT_2 = (PD_s - PD_p)/2$	(7)	nm

solutions. Mass recoveries were measured by comparing the absorbance at 220 nm of a standard protein solution before and after chromatography of a given quantity. Recovery of activity was determined using enzymes and measuring activity before and after chromatography.

Bonded layer properties were defined and measured as shown in Tables 4–7.

2.2.1. Column "titration" method. This method is used to determine the carboxyl ligand density of bonded phases under dynamic conditions similar to those used in ion-exchange chromatography of biopolymers. A high-performance liquid chromatography (HPLC) column is packed with bonded phase, equilibrated with buffer A (25 m*M* KH_2PO_4, pH 4.5), and pH measured at the column outlet. When the pH is constant, buffer B (25 m*M* KH_2PO_4, pH 7.0) is pumped through the column while pH is monitored until a short time after the breakthrough point (where pH increases to 7). Fig. 1 shows a typical pH–time profile for a packed column of BakerBond Wide-Pore CBX, 40-μm bonded phase. The time elapsed from zero (when buffer B first enters the column) to the inflexion point is an empirical measure of the relative carboxyl group content of that lot of bonded phase.

TABLE 6

DEFINITIONS OF LIGAND DENSITIES IN BAKERBOND WIDE-PORE BONDED PHASES

Phase types	Ligand density	Units
Alkyl, hydrophilic polymer, anion or cation exchangers, hydrophobic interactors	$\%C \cdot 10^3/1.2 \cdot SA \cdot$ carbons per ligand chain (eqn. 3)	μmol of ligand per m^2
Weak cation exchangers	Carboxyl groups per molecule of hydrophilic polymer	None
	Carboxyl groups per m^2	μmol COOH per m^2
Weak anion exchangers	Anion groups per m^2	μmol NH per m^2
Mixed strong/weak cation exchangers	Carboxyl + sulpho groups per m^2	μmol COOH + SO_3 per m^2
Hydrophobic interactor	Propyl groups per m^2	μmol C_3 per m^2

TABLE 7

METHODS OF CALCULATING LIGAND DENSITY FOR WEAK CATION EXCHANGERS FROM ELEMENTAL ANALYSES

Type of ligand density	Equation[b,c] (derivations given in Appendix 2)	
Carboxyl groups per ligand[a]	$v = \frac{n}{4}\frac{(C_p - C_h)}{C_h}$	(8)
μmol carboxyl per m^2	$\frac{10^3\ C_h\ v}{1.2\ n\ SA}$	(9)
or		
μmol carboxyl per m^2	$\frac{(C_p - C_h)\ 10^4}{48\ SA}$	(10)

C_p = %C in bonded phase
C_h = %C in hydrophilic polymer clad silica
n = carbons per ligand
v = carboxyl groups per ligand
SA = specific surface area of hydrophilic polymer – clad silica

[a] Ligand here means the reactive hydrophilic polymer chain.
[b] For each four carbons added to the hydrophilic polymer, one carboxyl is formed.
[c] Eqns. 9 and 10 are equivalent. Eqn. 10 is simpler since a knowledge of v and n is not required.

2.3. Results

Data presented in this review were obtained from either experimental lots of bonded phase (Tables 8–10) or production lots (Tables 11–15, 19, 20 and 21). Experimental lots were chosen at random for the relevant tables. Data from production batches are those gathered from every lot made over the past two years (June 1988 to June 1990 approximately). Calculated and measured values of the properties in Tables 5 and 7 for experimental batches of bonded phases are given in Tables 8–10.

Values of elemental analyses, silica surface areas and carbon and nitrogen ligand densities for multiple production batches of selected bonded phases are given in Tables 11 and 12.

Carboxyl functional group ligand densities and related parameters for consecutive lots of production batches of Bakerbond Wide-Pore CBX, 5 μm, are given in Table 13.

Major pore characteristics for several lots of silicas use in bonded phase production are listed in Tables 14 and 15.

A definition of terms is given in Appendix I. Other definitions can be found in Tables 4 and 6. Appendix 2 contains derivations of eqns. 2–10.

3. DISCUSSION

There are many techniques that can be used to characterize silica and its bonded phases. Among them are spectroscopic (NMR, Fourier transform IR, electron spectroscopy for chemical analysis, for example), thermogravimetric, porosimetric, adsorptive, chemical and chromatographic methods [6,7]. This discussion will be

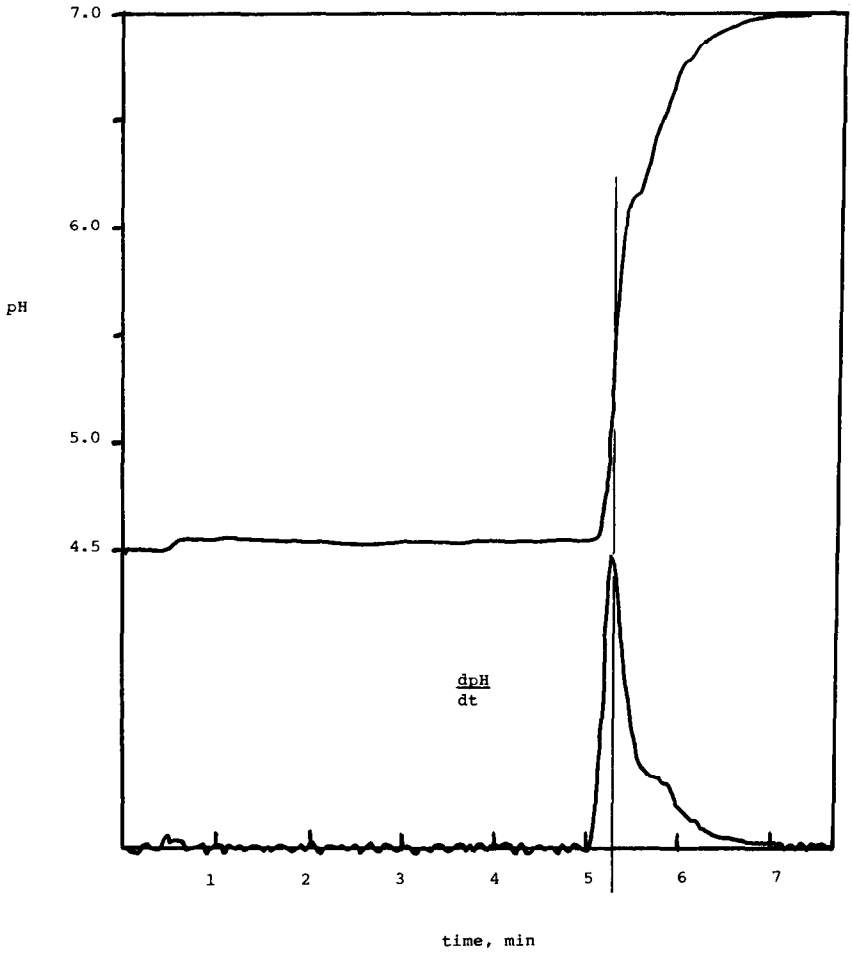

Fig. 1. pH–time (t) and dpH/dt–time relationships for the eluent from a packed column (250 × 4.6 mm) of BakerBond Wide-Pore CBX, 40 μm, as bonded phase is titrated.

TABLE 8

VALUES OF PHYSICAL PROPERTIES OF EXPERIMENTAL BAKERBOND WIDE-PORE BONDED PHASES

Property	Unit	5-μm PEI	5-μm CBX	5-μm C_{18}	5-μm ABx
PD_s	nm	27.5	27.5	23.5	23.5
PD_p	nm	25.8	25.0	17.3	20.9
PV_s	ml/g	0.48	0.48	0.69	0.52
PV_p	ml/g	0.39	0.34	0.37	0.38
SLV	mm^3/m^2	1.29	2.1	2.6	2.0
LD	g/ml	0.71	0.63	0.33	0.66
LT_1	nm	1.29	2.1	2.6	2.0
LT_2	nm	0.8	1.3	3.1	1.3
%Organic		6.42	8.8	10.4	9.3
SA_s	m^2/g	70	66	123	70
SA_p	m^2/g	65	60	80	62

TABLE 9

VALUES OF CARBOXYL GROUPS REACTED PER MOLECULE OF THE HYDROPHILIC POLYMER[a] FOR EXPERIMENTAL LOTS[b] OF BAKERBOND WIDE-PORE CBX

Lot. No.	Pore size (PD_s)	Surface area (SA_s)	Particle size (μm)	Polymer		CBX (%C)	Carboxyl groups
				%C	%H		
74	500	66	5	3.64	0.8	6.16	5.19
50	500	95	40	3.75	0.9	6.52	5.54
51	1000	55	40	1.98	0.5	3.42	5.46
53	300	185	40	5.5	1.3	9.40	5.32
70	500	75	15	4.62	1.1	7.14	4.09
25	500	99	30	6.88	1.8	10.81	4.28
161	275	204	40	6.88	1.8	11.86	5.43
620	300	104	5	3.16	0.7	5.65	5.91

[a] Calculated from equation 8.
[b] The above bonded phases were prepared on eight different silicas.

TABLE 10

CARBOXYL LIGAND DENSITIES[a] FOR EXPERIMENTAL BATCHES[b] OF BAKERBOND WIDE-PORE CBX

Lot No.	Nominal silica pore size (nm)	Surface area (m^2/g)	Ligand density (μmol/m^2)	
			Method 1	Method 2
25	50	99	8.26	8.27
50	50	95	6.07	6.07
51	100	55	5.46	5.46
53	30	185	4.39	4.39
70	50	75	7.00	7.00
74	50	66	7.95	7.95
161	27.5	204	5.09	5.09
620	30	104	4.99	4.99

[a] Method 1 used eqn. 9 and method 2 used eqn. 10.
[b] The above bonded phases were prepared on eight different silicas.

limited to information gathered from porosimetry measurements, chemical analysis and chromatographic analysis, as these tests are routinely carried out on all of our silicas and bonded phases, whether they are experimental or production batches.

3.1. Physical properties and characterization of porous silica

3.1.1. Particle size distribution. A narrow particle size distribution can be obtained either during the manufacture of silica or by sizing after manufacture or both. All processes are amenable to a significant amount of control, although no truly monodisperse silicas have been synthesized.

It is generally considered that maximum efficiency and minimum backpressure

TABLE 11

CARBON AND NITROGEN LIGAND DENSITIES AND C/N RATIOS FOR PRODUCTION BATCHES OF 5-μm BAKERBOND WIDE-PORE PEI AND CBX BONDED PHASES

BakerBond Wide-Pore PEI							
Lot No.	275	175	213	134	249	103	240
Silica surface area (m^2/g)	116	116	95	116	119	92	119
%C	6.52	5.81	4.86	6.54	5.90	5.35	5.96
Carbon Lig. D ($\mu mol/m^2$)	46.8	41.7	42.6	46.9	41.3	48.5	41.7
%N	3.02	2.74	2.26	3.02	2.72	2.50	2.76
Nitrogen Lig. D ($\mu mol/m^2$)	18.5	16.8	17.0	18.5	16.3	19.4	16.5
C/N (w/w)	2.16	2.12	2.15	2.17	2.17	2.14	2.16
BakerBond Wide-Pore CBX							
Lot. No.	243	271	212	244	273	221	272
Silica surface area (m^2/g)	116	116	95	116	119	92	119
%C	10.48	9.68	7.96	10.63	9.70	8.67	9.65
Carbon Lig. D ($\mu mol/m^2$)	75.3	69.5	69.8	76.3	67.9	78.8	67.5

TABLE 12

OCTADECYL LIGAND DENSITIES ON PRODUCTION BATCHES OF BAKERBOND WIDE-PORE C_{18} 5-μm BONDED PHASE

	Batch								
	220	127	126	116	110	101	113	096	097
Silica surface area (m^2/g)	78.0	76.7	78.0	78.0	78.0	76.7	85.0	85.0	85.0
%C	6.80	7.30	7.18	8.00	7.63	7.89	7.95	7.98	8.06
Carbon Lig. D ($\mu mol/m^2$)	72.0	79.3	76.7	85.4	81.5	85.7	77.9	78.2	79.0
C_{18} Lig. D	4.0	4.4	4.3	4.7	4.5	4.8	4.3	4.3	4.3

TABLE 13

CARBOXYL GROUP LIGAND DENSITIES IN CONSECUTIVE LOTS OF BAKERBOND WIDE-PORE CBX BONDED PHASE

	Lot No.						
	212	221	243	244	271	272	273
Silica surface area (m^2/g)	95	92	116	116	116	119	119
Hydrophilic polymer clad silica (HPCSi) surface area (m^2/g)	81	78	99	99	99	102	102
%C in CBX (C_p)	7.96	8.67	10.48	10.63	9.68	9.65	9.70
%C in HPCSi (C_h)	4.86	5.35	6.54	6.54	5.81	5.96	5.90
Carboxyl groups per hydrophilic polymer chain (v)	4.78	4.65	4.52	4.69	5.00	4.64	4.8
Carboxyl ligand density μmol of $COOH/m^2$, calculated from eqn. 9	7.97	8.86	8.29	8.61	8.15	7.53	7.7
Carboxyl ligand density μmol $COOH/m^2$, calculated from eqn. 10	7.97	8.86	8.29	8.61	8.15	7.53	7.7

TABLE 14

MAJOR PORE CHARACTERISTICS OF CONSECUTIVE LOTS OF 5-μm WIDE-PORE (NOMINALLY 30 nm) SILICAS USED IN BAKERBOND WIDE-PORE BONDED PHASES

Lot No.	Surface area (m^2/g)	Pore volume (ml/g)	Pore diameter (nm)
201	117	0.87	26.3
423	120	0.95	26.0
705	119	1.03	26.2
316	104	1.00	28.3
707	116	0.87	27.5

TABLE 15

MAJOR PORE CHARACTERISTICS OF CONSECUTIVE LOTS OF 40-μm WIDE-PORE SILICAS USED IN BAKERBOND WIDE-PORE BONDED PHASES

Lot No.	Surface area (m^2/g)	Pore volume (ml/g)	Pore diameter (nm)
1268	310	1.78	254
1487	280	1.78	230
2346	283	1.73	244
2162	293	1.78	243
2452	287	1.66	257

is obtained when particle size distribution is narrowest [8]. Our laboratories have distribution specifications for all silicas we use which significantly restrict fines and large diameter particles. Fig. 2 illustrates several particle size distributions for our silicas.

3.1.2. Pore size and pore size distribution. For analytical applications, nonporous particles are sometimes used in the HPLC of biomacromolecules [9]. However, porous particles are still the predominant type of packing matrix used in biochromatography [10–13]. The pore diameter, pore depth, pore shape and the distribution of these, are parameters which influence chromatographic properties and the corresponding bonded phases[6].

A pore diameter of 20–30 nm is accepted as being required for optimum resolution, capacity and recovery of most proteins in the molecular weight range 10 000–200 000 dalton. For proteins up to $1 \cdot 10^6$ dalton a pore size of about 50 nm or larger is preferable. For steric reasons the larger pore is required to enable a biopolymer to gain access to all binding sites on the surface of a bonded phase. This access maximizes binding capacity and minimizes contributions of steric exclusion to the separation mechanism. Furthermore, the large pore diameter increases the rate of mass transfer, which is especially important for large molecules. A larger pore diameter of the substrate silica is also required, since this parameter decreases after the bonded layer is attached. This subject is discussed further in Section 3.3.1.

A single number value for commonly-quoted pore diameters can often be

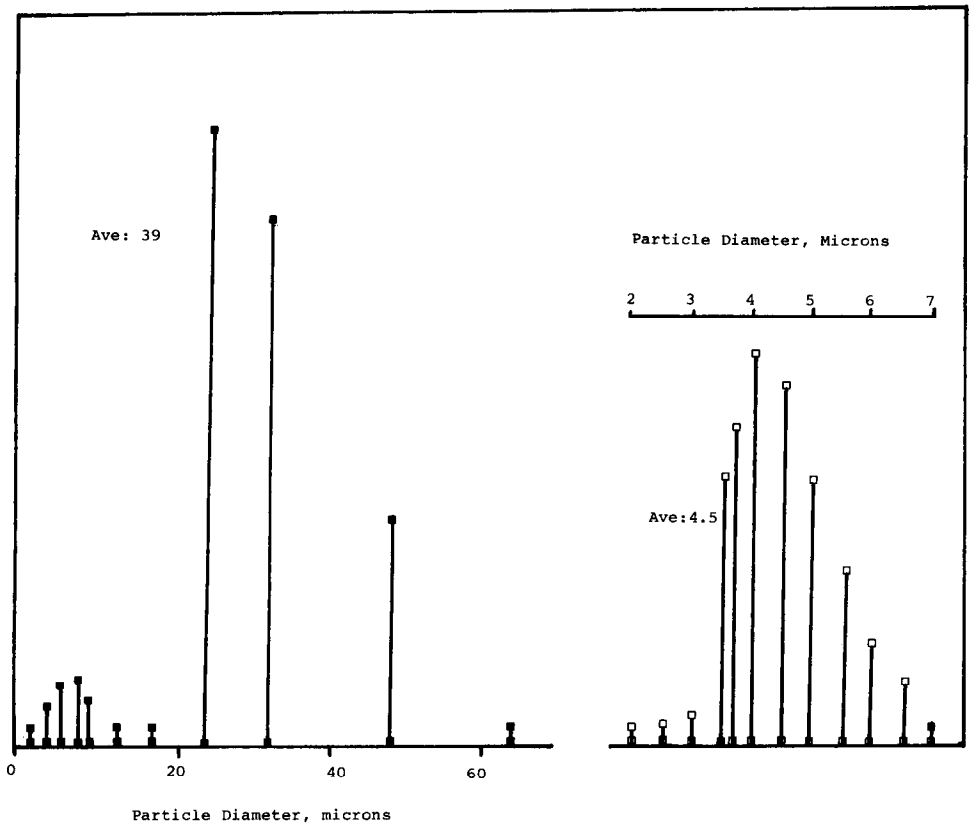

Fig. 2. Particle diameter distributions of two types of silica.

misleading, and the way it is measured will determine its value. For example, pore diameters obtained from size exclusion curves or calculated from measured values of pore volume and surface area (see eqn. 11) are single number averages. On the other hand pore-diameter distributions can be obtained using techniques such as mercury porosimetry. This technique is preferred and used routinely in our laboratories for our wide pore silicas, since it gives a more complete picture of how pores are distributed in these silicas and their bonded phases.

$$PD_s = \frac{PV_s}{SA_s} \cdot 4 \cdot 10^3 \tag{11}$$

In this technique mercury is forced into pores within the silica, under pressures whose magnitudes are related to pore diameter.

The pressure–pore diameter relationship is expressed in the Washburn equation:

$$P \cdot PD_s = -4\, l \cos \theta \tag{12}$$

where P is the applied pressure, PD_s the pore diameter, l the surface tension of mercury (480 dynes/cm) and θ the contact angle on silica (140°). Eqn. 12 can be simplified to

$$P \cdot PD_s = 213.4 \text{ p.s.i. } \mu m \tag{13}$$

Thus, the volume of mercury absorbed (V) can be expressed as a function of pressure (P) or pore diameter (PD_s). Alternatively the slope of the volume–pressure curve (dV/dP) can be plotted against the pore diameter. Finally the volume distribution function $D_v(d)$ calculated from

$$D_v(d) = \frac{P}{PD_s} \cdot \frac{dV}{dP} \tag{14}$$

can be plotted against pore diameter. This relationship is a very useful one to illustrate the pore diameter distribution. Fig. 3 contains plots of V *versus* PD_s. dV/dP *versus* PD_s and $D_v(d)$ *versus* PD_s, for a nominally 20-nm (200-Å) silica. Such pore size distributions may be broad or narrow, symmetrical or unsymmetrical. Figs. 4 and 5 shows $D_v(d)$ *versus* pore diameter plots for several silicas used by our laboratories in research and manufacturing. They are considered to have a moderately narrow range of pore diameters, without a proportionately large number of wide pores or narrow pores.

The data obtained from the two types of physical measurements that are made, namely pressure and volume, can ultimately be used to calculate several types of pore–diameter distributions. These include pore volume–pore diameter, pore surface area–pore diameter and volume distribution function– pore diameter relationships. A single number value for pore diameter is then calculated from one of the above

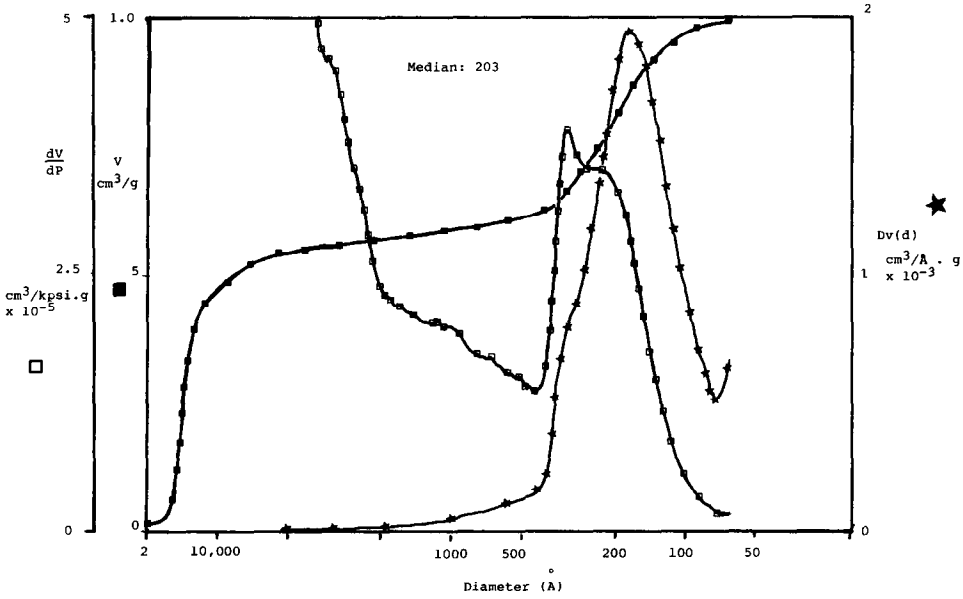

Fig. 3. Relationships of V, dV/dP and $D_v(d)$ to pore diameter (PD_s) for a nominally 200-Å pore silica.

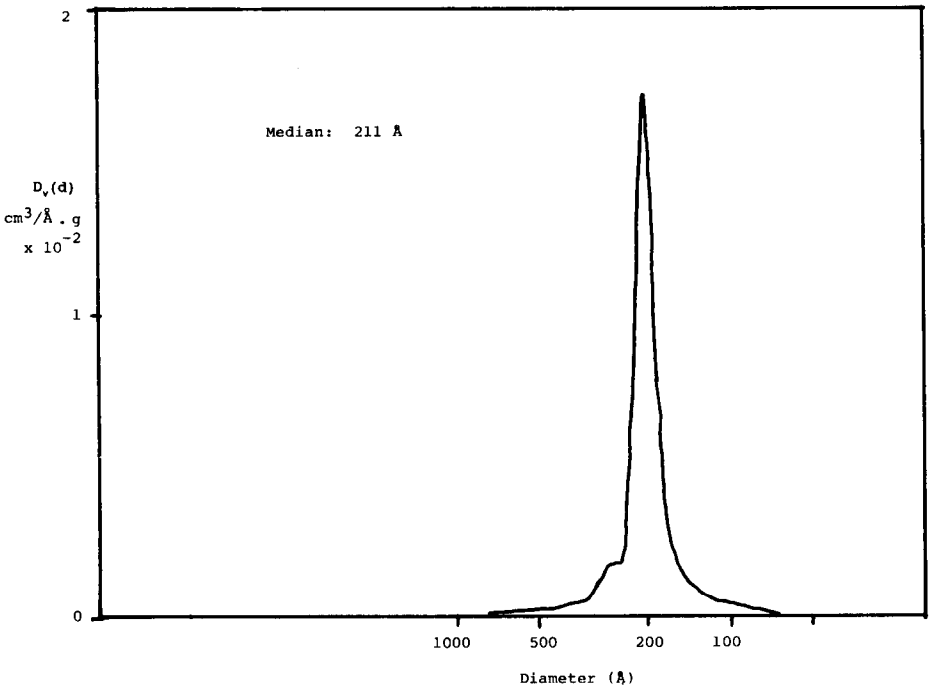

Fig. 4. Relationships of $D_v(d)$ to PD_s for a nominally 30-nm silica.

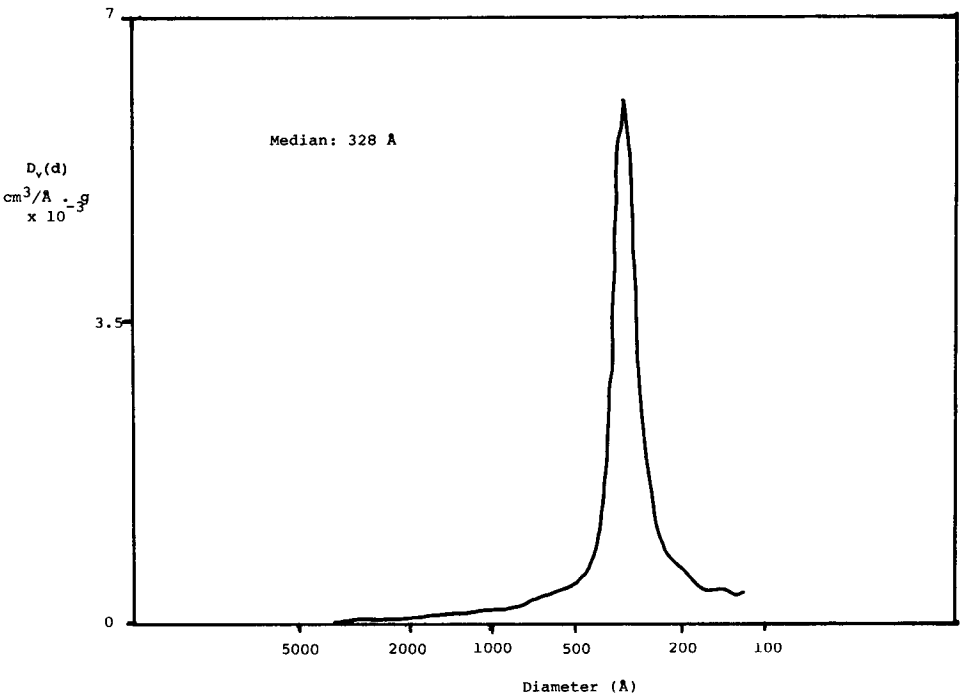

Fig. 5. Relationship of $D_v(d)$ to PD_s for a nominally 50-nm silica.

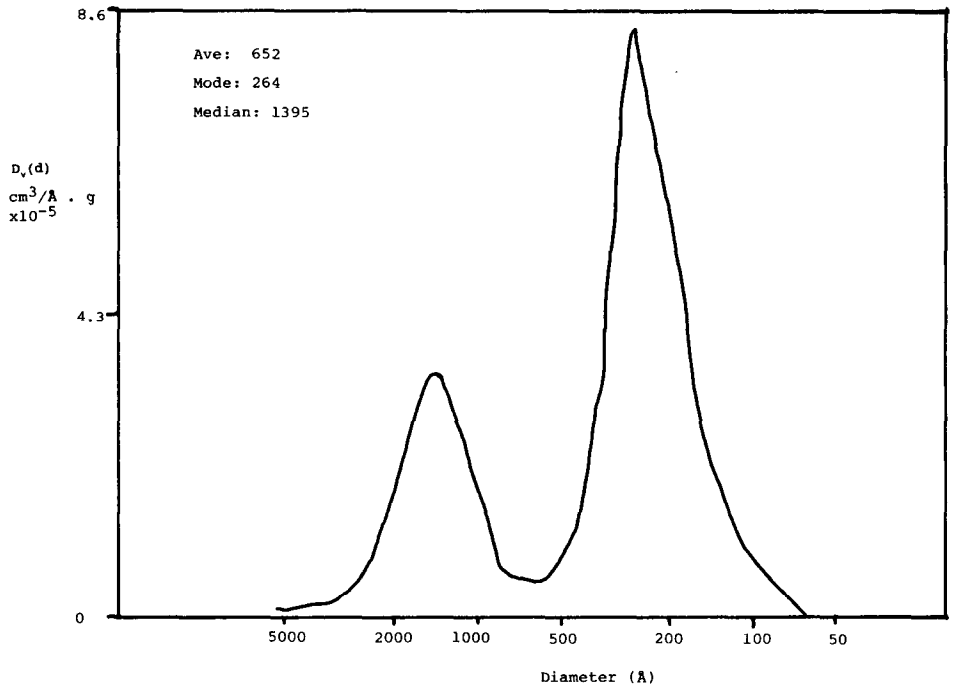

Fig. 6. Relationship of $D_v(d)$ to PD_s for a nominally 50-nm silica, illustrating biomodality.

distributions. This number may be a mean (or average), defined as the sum of values divided by the number of values. The mode is defined as the value occurring most frequently and the median is the mid-point of the population. For the purposes of this review, the median number will be used throughout, except where indicated.

Occasionally pore size distributions are bimodal; in other words show two distinct populations of pores distributed about two maxima. Fig. 6 gives such plots for a sample of wide-pore silica. Silica preferred in our laboratories will generally have

TABLE 16

PORE DIAMETERS, PORE VOLUMES AND SURFACE AREAS FOR SEVERAL SILICA GELS

These values are nominal values supplied by the manufacturer.

Manufacturer	Silica type	Pore diameter (nm)	Pore volume (ml/g)	Surface area (m^2/g)
Davison	Davisil	6.0	0.75	500
	Davisil	27.5	1.70	250
Asahi glass	MS Gel	12.0	0.90	300
DuPont	Zorbax	11.5	0.90	315
Separations group	Vydac	24.0	0.7	115
Shandon	Hypersil	30.0	0.6	50
Exmere	Exsil	30.0	0.8	100
Crosfield	Sorbsil	50.0	1.5	110

monomodal, narrow, symmetrical pore size distributions (see Fig. 4). There is general agreement that such silicas will demonstrate the best peak shape in terms of width and symmetry.

The data in Figs. 3–5 describe properties of the substrate only. After bonding, pore diameters decrease. This topic is discussed in section 3.3.

3.1.3. Pore volumes and surface areas. Silicas are manufactured in a broad range of pore diameters, pore volumes and surface areas. Table 16 includes data for these parameters from several sources. The simple relationship (eqn. 11) amongst the pore diameter, pore volume and surface area, is quite accurate even when different silica manufacturers are compared. Fig. 7 shows a plot of PD_s (equation 11) *versus* PD_s (average from mercury porosimetry) for a wide range of silicas from different manufacturers.

In general, our laboratories prefer that for a given pore diameter, the maximum surface area is available for maximum binding capacity. This generally means a high pore volume and thus a potential for lower than normal particle strength. However, mechanical strength is very variable from one silica manufacturer type to another.

3.1.4. Reproducibility of silicas. Lot-to-lot consistency of pore diameter, pore volume and surface area, is critical if the corresponding bonded phases are to show

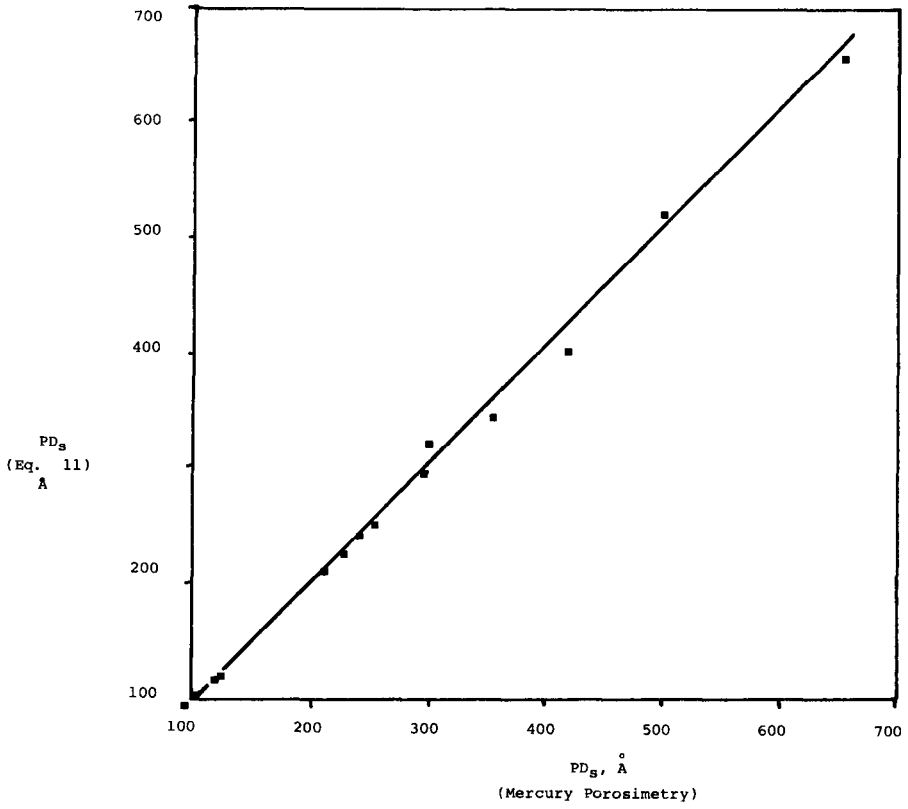

Fig. 7. Relationship between pore diameter calculated from eqn. 11 and the average pore diameter measured by mercury porosimetry.

reproducibility. Tables 14 and 15 contain lot history data from measurements on several lots of various silicas we employ in bonded phase manufacture. The reproducibility is considered to be high, considering that these are newer wide-pore silicas which have greater variability in these physical properties than the more established narrow pore silicas.

3.2. Bonded phase design and synthesis

The chemistry of the modification of the silica surface developed in our laboratories, was chosen according to whether the bonded phase was non-polar on one hand or polar on the other. In each case the chemical processes were aimed at producing bonded phases that conformed as closely as possible to the ideals listed in Table 2.

Non-polar bonded phases were synthesized under polymer-forming conditions according to eqns. 15 and 16, using trifunctional silanes [14].

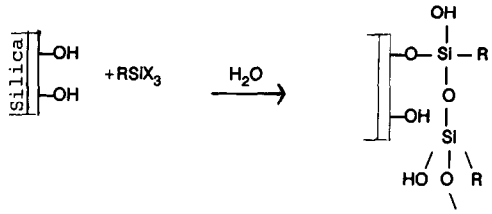

(15)

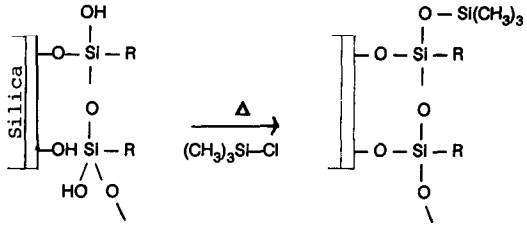

(16)

TABLE 17

BONDED PHASE LIGAND STABILITY AT VARIOUS pH VALUES WITH AND WITHOUT METHANOL

Bonded phase: *n*-butyl on 40-μm, 60-Å irregular silica; primary reaction: silylation with trichlorosilane; end-capping: trimethylsilyl group; initial analysis: 8.52%C, 2.05%H; treatment: with various solutions, 50°C for 125 h; 1 g bonded phase in 15 ml solution. Elemental analyses are the average of duplicate measurements.

Analysis after treatment	Aqueous solutions			15 ml Aqueous + 3 ml methanol		
	1% H_3PO_4 (pH 3)	HCl (pH 3)	pH 10	1% H_3PO_4 (pH 3)	HCl (pH 3)	pH 10
%C	8.36	8.28	8.32	7.97	7.90	8.35
%H	2.03	2.02	2.05			
Loss (%C)	0.18	0.25	0.21	0.56	0.64	0.18

The resulting hydrophobic surfaces are known to be hydrolytically stable [15,16], and tests in our laboratories confirmed this behavior (see Table 17). The access of small molecules to any silanols within or underlying such polymeric bonded coatings has been shown by Nendek *et al.* [17] to be one tenth of that with bonded phases prepared from monofunctional silanes. Furthermore, the rate of equilibration of a polymer phase with the mobile phase is more rapid than with a monomeric phase [18]. It was for these three reasons that we chose trifunctional silanes to prepare our bonded phases.

Polymeric bonded phases are however, more difficult to prepare reproducibility because of the multiple reaction products of the silylation reaction (see eqns. 15 and 16). Furthermore, it is believed that the slower rates of adsorption and desorption of analyte molecules at the surface of such polymeric phases reduces mass transfer rates and consequently column efficiency. Work in our laboratories has addressed these perceived limitations, and a discussion of this is given in section 3.3.

The polyethyleneimine bonded phase was synthesized according to the reaction in eqn. 17. The preparation of the weak cation exchangers, hydrophobic interactor and strong cation exchanger are given elsewhere [19–21].

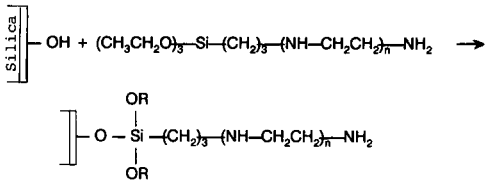

(17)

All bonded phases prepared in our laboratories have, in one way or another, polymeric surfaces (see eqns. 15, 16, and 17). The nature of the binding and the diffusion of biopolymers to and from this surface will be influenced by several of its properties:

(1) The distribution of functional groups across the surface.

(2) The new pore-size distribution, changed from that of bare silica as a consequence of the bonded layer, and

(3) The flexibility of the polymer chains in the bonded surface, which will provide a unique set of attachment points for the biopolymer, and will therefore influence selectivity.

Control over and measurement of the dimensions and properties of the bonded layer, is therefore a key to influencing many of the chromatographic properties of the bonded phase. These aspects of bonded phase synthesis are described next in section 3.3.

3.3. Characterization of bonded phases

3.3.1. Physical methods. For monolayers, ligand density (Lig. D) is a measure of the number of ligands (functional groups), usually expressed as micromoles, per square meter. However, for polymeric phases prepared from trifunctional silanes, ligand density is a more complex somewhat artificial concept. Multilayers of functional groups build up the apparent ligand density, without necessarily increasing the crowding together of organic ligands. Furthermore, polymeric layers such as those

comprised of polyethyleneimine, extend into the pore by simple virtue of their polyelectrolyte nature [22]. In these cases (polymeric layers) the thickness, volume and density of the layer are additional useful properties which can be used to characterize the bonded phase. The properties were defined in Tables 4 and 6.

Table 8 lists values of SLV, LT and LD calculated from the equations in Table 5, for several Bakerbond Wide-Pore bonded phases.

The data in Table 8 show that, for example pore diameter, pore volume and specific surface area decrease on bonding: whether it is PEI bonding to silica or the weak carboxyl layer bonded to the hydrophilic polymer. Layer thicknesses are only in fair agreement (LT_1 compared to LT_2), indicating difficulties in interpreting the meaning of median pore diameter, (used for LT_2) and relating that to the more straightforward concept of pore volume used for LT_1 (see discussion on pore size distribution, section 3.1.).

The thickness of the C_{18} layer (2.6 nm from LT_1, Table 8) is significantly different from the value of 2.1 nm obtained by Sander and Wise [23] for a polymeric phase. This may be due to a different synthetic process and/or a pore size effect; although the difference in the environment of the BakerBond Wide-Pore sample (mercury vapor) and the Sander and Wise sample (methanol), may invalidate any close comparison.

It is useful to contrast the effect on the properties of bare silica of the C_{18} group with the PEI group. The pore diameter decreases much more with the C_{18} phase (6.2 nm *versus* 1.7 nm for PEI); pore volume decreases three times as much for the non-polar phase; layer volume is twice the magnitude; and the layer density is less than half that of the PEI phase. In other words there is more volume of a low density C_{18} phase, causing substantially reduced pore diameter and pore volume in the bonded phase. It is important to be aware of this when considering pore diameter effects upon chromatographic properties such as capacity, recovery and resolution.

The pore size distribution in a bonded phase should have approximately the same shape as that in the original silica, if the bonded layer has the same thickness at all surface locations. Fig. 8 compares pore-size distributions for a bare silica, with that of a corresponding bonded phase. It can be seen that although the maximum points on the curves are displaced, the general shape is the same for each plot. This is evidence that the silane in this case was bound evenly at all points on the silica surface.

Many of the physical properties described above (SLV, PV_p, LT for example) determine the basic chromatographic properties of bonded phases. This subject is discussed in section 3.3.3.

3.3.2. Chemical methods. Bonded phases may be characterized according to chemical properties such as their carbon, hydrogen or nitrogen content, hydrophobicity, and functional group content.

Elemental analysis. Tables 11 and 12 list the magnitude and variability of the carbon and nitrogen loadings for several BakerBond bonded phases. Since silica surface area may vary from lot to lot, (see Table 14 and 15, section 2), the consistency of manufacture of a bonded phase can only be gauged by taking this into account and comparing ligand densities. There are specifications for the permitted ranges of carbon and nitrogen ligand densities, which determine whether a production batch is accepted or rejected. All lots in Tables 11 and 12 were accepted for production. The C/N ratios are in particularly good agreement and reflect the consistency of the PEI-based silane (see eqn. 17).

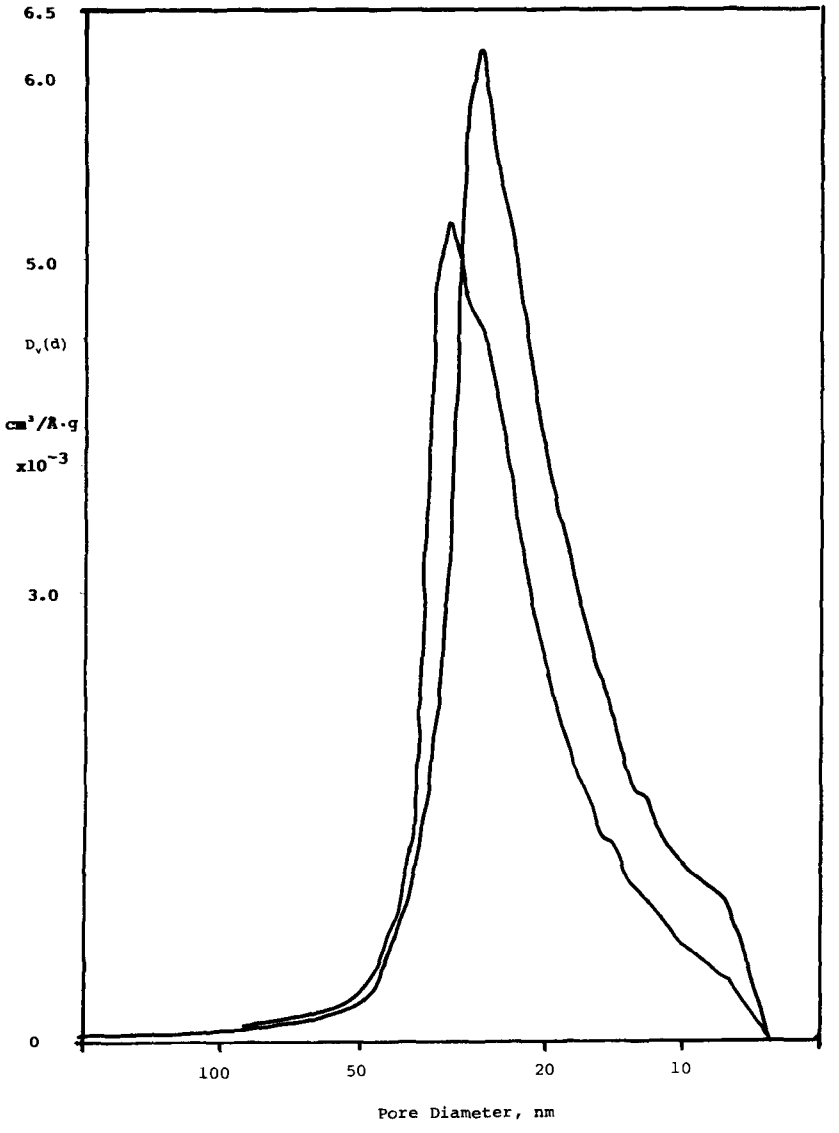

Fig. 8. Pore diameter distributions for a wide-pore silica and a corresponding bonded phase, illustrating their shape similarity.

Several batches of PEI and CBX were prepared on the same lot of silica, having the same surface area (for example Table 11, 116 and 119 m^2/g). Tables 11 and 12 show the moderate lot-to-lot variability in ligand densities obtained on a given silica.

Hydrophobic/hydrophilic character. The hydrophobic character of a bonded phase is difficult to quantify in general. It is important to obtain a qualitative measurement of hydrophobicity for ion exchangers, since certain biopolymers have a tendency to bind to the more hydrophobic matrices at the high ionic strengths used in

this form of chromatography [24,25]. The four major BakerBond ion exchangers (PEI, CBX, ABx and CSx, see Table 1) show negligible hydrophobic character. This is determined by the quantitative recovery at 2 *M* $(NH_4)_2SO_4$ of proteins that normally bind to the respective ion exchangers at low ionic strength. (These data are given in Table 18).

TABLE 18

MASS RECOVERIES OF PROTEINS FROM BAKERBOND WIDE-PORE ION EXCHANGERS UNDER HIGH IONIC STRENGTHS

Mobile phase was 2 *M* ammonium sulfate + 25 m*M* KH_2PO_4, pH 7.

Protein (from PEI)	Mass recovery (%)		Protein (from CSx)
	Bonded phase		
	PEI	Carboxy-sulfon (CSx)	
Calmodulin	>99	98	Bovine serum albumin
Myoglobin	>99	98	Myoglobin
Cytochrome *c*	>99	99	Cytochrome *c*
Lysozyme	>99	97	Lysozyme
α-Chymotripsinogen	>99	98	Carbonic anhydrase
		97	Human serum immunoglobulin G
		96	Mouse serum immunoglobulin G

The hydrophilic character in the BakerBond Wide-Pore ion exchangers is a property that was designed into these matrices. It depended upon the presence of the hydrophilic, reactive polymer (see eqn. 17), the absence of any PEI cross-linking [19], and the correct choice of reaction conditions. Of the last parameters, the solvent used during the grafting of the carboxyl groups into the hydrophilic polymer is important in eliminating the hydrophobity from the bonded phase. The reasons for this are unknown.

Ligand density. It is important to control and measure functional group content expressed as ligand density. This property may influence the chromatographic selectivity and binding capacity of a bonded phase. For example, the retention of hemoglobin on a BakerBond Wide-Pore CBX weak cation-exchange column is related to the carboxyl ligand density, as illustrated in Fig. 9. Retention of hemoglobin is effectively lost when the carboxyl ligand density drops below 6.5 $\mu mol/m^2$. Furthermore, the binding capacity of immunoglobulin G (IgG) polyclonal antibodies with BakerBond ABx, for example, is also related to the carboxyl ligand density of the bonded phase. Fig. 10 shows the relationship between this capacity and ligand density. Here, binding of the antibody is significantly compromised when ligand density drops below 4.3 $\mu mol/m^2$.

Thus a knowledge of ligand density is important not only to meet performance specifications (capacity, selectivity), but also to measure reproducibility.

Ligand densities in principal refer to the moles of a specific functional group per unit area of bonded phase surface. The concept is relatively straightforward for

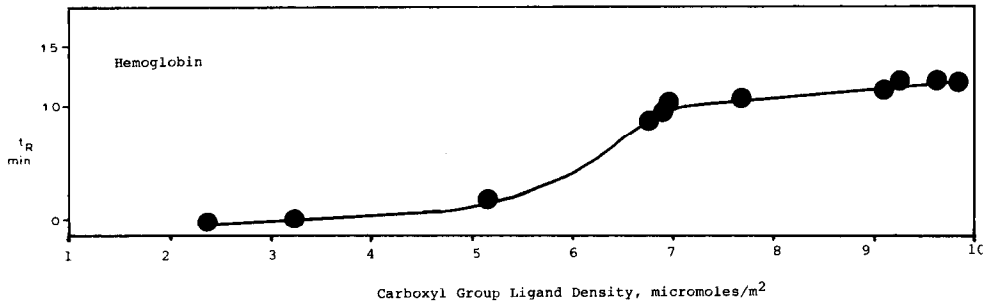

Fig. 9. Retention of hemoglobin as a function of carboxyl group ligand density in BakerBond Wide-Pore CBX (40 μm) weak cation exchanger. Conditions: 250 × 4.6 mm column. Buffer A: 25 m*M* 2-(N-morpholino)ethanesulfonic acid (MES), pH 5.8. Buffer B: 1 *M* sodium acetate, pH 5.8. Gradient: 100% A to 100% B over 45 min. Flow-rate: 3 ml/min. Hemoglobin injected: 0.75 mg. t_R = Adjusted retention time.

non-polar surfaces such as the C_{18} phases, where the octadecyl silyl group is intact and unchanged. Ligand densities for nine production lots of a wide pore C_{18} are given in Table 12. The agreement among the values is excellent, with an average of 4.23 μmol/m^2. This value is significantly higher than the maximum value for a monomeric

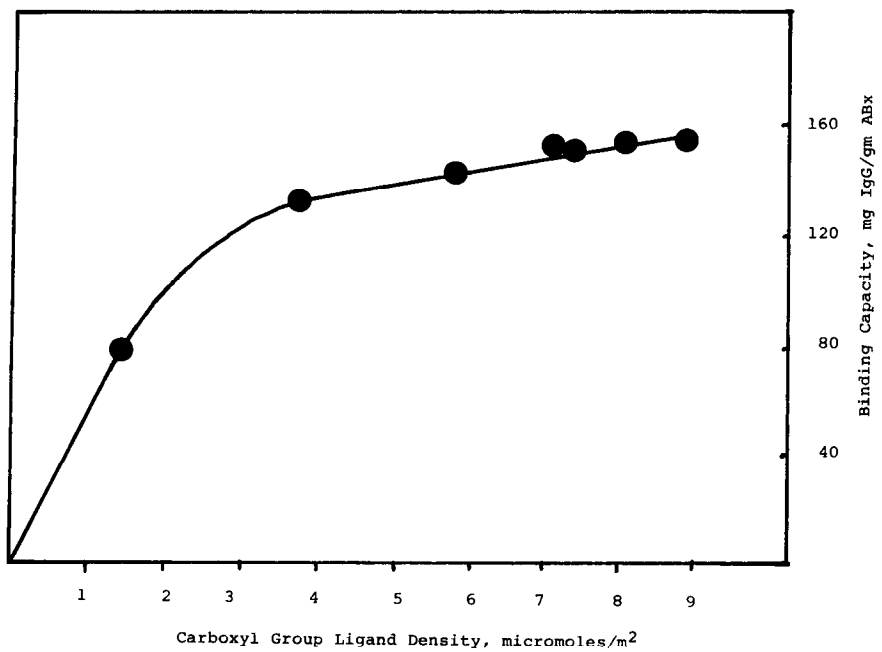

Fig. 10. Binding capacity of an IgG polyclonal antibody in BakerBond ABx as a function of carboxyl ligand density. Binding capacities were measured by allowing 100 mg of the bonded phase to become saturated with mouse polyclonal antibody from 20 mg of protein in 20 ml of a buffer of 25 m*M* MES, pH 5.4. The quantity of antibody remaining in solution (after filtration and washing of the adsorbent with the buffer) was determined spectrophotometrically. The quantity bound was calculated by difference.

TABLE 19

ELEMENTAL ANALYSES, SILICA SURFACE AREAS AND LIGAND DENSITIES FOR HYDROPHILIC POLYMER-CLAD SILICA USED TO PREPARE BAKERBOND WIDE-PORE CBx

Lig. D calculated from eqn. 3, Table 5.

Lot. No.	%C	SA_s (m^2/g)	Lig. D ($\mu mol/m^2$)
419	5.34	117	1.27
520	5.21	117	1.24
714	5.32	120	1.23
130	6.42	116	1.54
123	5.86	119	1.37
124	5.96	119	1.39
618	4.86	95	1.42
619	4.86	95	1.42
612	4.84	92	1.46

C_{18} chain achieved by Kirkland *et al.* [26] (2.69 $\mu mol/m^2$). In fact the ligand density of 4.23 is in good agreement with the value of 4.1 found by these authors [26] for the small trimethylsilyl group. The reason for the large apparent ligand densities is the polymeric nature of the BakerBond Wide-Pore non-polar surface. The polymeric layer will be thicker than the monomeric layer, by a factor of about 4.23/2.69 or 1.6. Using a layer thickness of 1.7 nm for a monomeric C_{18} phase (Sander and Wise [23]), this factor predicts a thickness of 2.7 nm for the BakerBond polymer layer. This is in excellent agreement with the value of 2.6 nm obtained from mercury porosimetry methods (see the value of LT_1 for C_{18} in Table 8).

Ligand density is also a simple concept for the hydrophilic polymer-clad silicas, since the polymer is well characterized and has the same molecular weight from batch-to-batch.

If we assume that the hydrophilic polymer has 30 carbons per chain (*versus* 18 for the octadecyl group), then ligand densities for the corresponding bonded phase can be calculated from %C and specific surface areas of the silica substrate. Table 19 lists the values of these parameters for production lots of the hydrophilic polymer-clad silica. The ligand densities given in this table are in good agreement, and are significantly lower than those that would be estimated for an alkyl chain having 30 carbons. The reason for this is that the hydrophilic polymer molecule is branched and consequently takes up more space on the silica surface, than an *n*-alkyl group.

For those bonded phases where a new functional group is added to the hydrophilic polymer surface, the idea of ligand density is clear, but it's control and measurement may be difficult. These phases include the strong and weak cation exchangers and the hydrophobic interactor (see Table 6).

For the weak cation exchangers (where the ligand is carboxyl) we have developed several methods to calculate ligand density. The methods are as follows:

(A) Measurement of carbon uptake as carboxyls are added (see calculation methods in Table 7, and results in Tables 9, 10 and 13).

(B) Colorimetric reaction with the carboxyl group (see section 2.1, methods and results in Table 21).

In addition to these quantitative methods, we have developed a column "titration" method, which gives a qualitative estimate of ligand density. (This method was described in section 2.1).

Method A. The number of carboxyl groups reacted per hydrophilic polymer chain, v, (calculated from eqn. 8) is another chemical parameter in which we seek to achieve reproducibility. Production lot values of v given in Table 13 show excellent consistency. This parameter, together with the ligand density of the hydrophilic polymer, determine the overall carboxyl ligand density. This last parameter can be calculated from eqn. 9, using values of v calculated from eqn. 8; or calculated more simply from eqn. 10, in which neither v nor n (carbons per ligand chain) are required.

Tables 10 and 13 list values of carboxyl ligand densities for experimental lots of BakerBond Wide-Pore CBX on various silica types, and for production lots of this bonded phase on a single silica type. Lot-to-lot agreement is excellent, with an average of 8.16 μmol/m^2. This value is considerably higher than that for a trimethylsilyl or octadecylsilyl bonded phase, (4.5 μmol/m^2, Table 12) and is due to the fact that five carboxyl groups on average are reacted with each hydrophilic polymer chain. Under use conditions the ionized carboxyl groups form a surface with a high charge density. If all carboxyl groups were ionized, this property would be 0.82 negative charges per nm^2 or 0.82 charges per 100 Å^2.

Method B. This method has been shown by Ngo [5] to give a measurement of the carboxyl ligand density in solid-phase supports, in units of μmol/ml. We routinely measure carboxyl group content using the same procedure, and results are presented in Table 20. For comparison, carboxyl ligand densities calculated from eqn. 10 are given.

The two methods give significantly different results, with no obvious correlation. Method A is simpler and relies on more accurate data (microanalysis of %C) and therefore, although more indirect than method B, is considered to be the more accurate. Ligand density reproducibility can be seen to be excellent with method A.

The difficulty in achieving precise agreement amongst indirect and direct methods for determining ligand densities, is due to the three-dimensional nature of the bonded layer. Ligands in such layers may be more or less accessible to interactive

TABLE 20

VALUES OF C_h, C_p AND CARBOXYL LIGAND DENSITIES CALCULATED BY METHODS A AND B FOR BAKERBOND ABx, 40-μm PRODUCTION LOTS

C_h = %C on hydrophilic polymer–clad silica; C_p = %C on BakerBond ABx; SA_p = surface area of hydrophilic polymer-clad silica. Method A: using eqn. 10; method B: using the colorimetric method of Ngo [5].

Lot. No.	C_p	C_h	SA_p	Lig. D (μmol/m^2)	
				Method A	Method B
2691	11.7	7.1	139	6.89	7.91
3091	12.1	7.5	139	6.89	9.35
3382	11.4	7.0	139	6.59	9.35
3718	11.4	6.7	139	7.04	9.35
4820	11.5	6.8	139	7.04	5.76

species (reactants, biopolymers for example) due to steric effects which control access. Elemental analysis characterizes the entire bonded layer. On the other hand measurements of ligand densities through processes involving the diffusion of molecular species to and sometimes into the bonded layer, may be inaccurate since the whole layer may not take part in the adsorption.

3.3.3. Chromatographic methods. The adjusted retention time, t_R, can be considered to be an approximate measure of the time spent by a component immobilized in and on the bonded layer. Thus its magnitude will depend on the specific layer volume (SLV) and other properties of the layer such as its hydrophobic character and degree of solvation. Hydrophobicity will be related in a complex way to the degree of polymerization (Sander and Wise α_{PAH} value, see below). The degree of solvation of the bonded layer will influence the solubility of a compound in the phase. Non-polar polymeric layers have been shown to be less solvated than monomeric layers (Sander and Wise [23]), and consequently they are less polar and will bind polar compounds

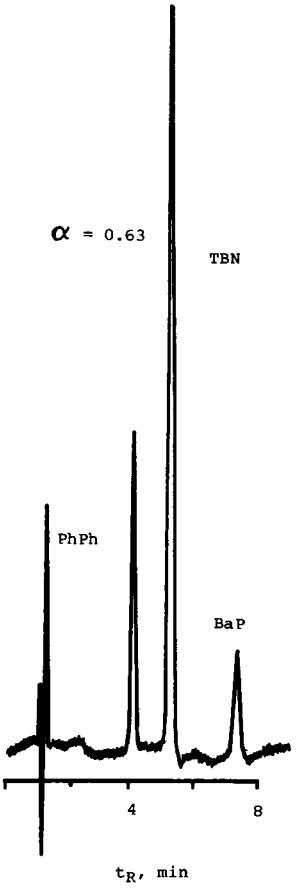

Fig. 11. Elution order of PhPh, TBN and B*a*P on a typical BakerBond Wide-Pore C_{18}, 5-μm column. Mobile phase: acetonitrile–water (85:15). The value of the separation factor α_{PAH} (see eqn. 18) is 0.63 for this lot of bonded phase.

less strongly. This partly explains the observations of Scott and Simpson [18] regarding the more rapid re-equilibration of non-polar polymeric packings, since less time is involved in solvent exchange between the bonded layer and the pore volume for these phases, in comparison to the mono-layered packings.

These and other chromatographic properties such as capacity factor (k'), separation factor (α) and ultimately resolution, are therefore intimately related to the physical properties described in section 3.3.1.

All Wide-Pore C_{18} bonded phases are subjected to an additional characterization method developed by Sander and Wise [27]. In this test, a packed column, equilibrated with an 85/15 acetonitrile–water (85:15) mobile phase, is injected with a mixture of phenanthro[3,4-*c*]phenanthrene(PhPh), tetrabenzonaphthalene (TBN) and benzo[a]pyrene (B*a*P). The elution order of these compounds depends upon the polymeric nature of the ligand. The bonded phases developed at J.T. Baker contain polymeric silanes bound to silica, and consequently the three probe compounds elute in the order PhPh, TBN, B*a*P (see Fig. 11). The separation factor α_{PAH} is defined in eqn. 18 and is held within the range 0.5 to 0.8. Separation factors for multiple batches, illustrating our control over this parameter, are given in Table 21. This factor is very sensitive to reaction conditions, and is a quantitative measure of the degree of polymeric character in the phase which we wish to control.

$$\alpha_{PAH} = \frac{k' \text{ (tetrabenzonaphthalene)}}{k' \text{ (benzo[}a\text{]pyrene)}} \tag{18}$$

This separation factor can be altered at will depending on the polymeric character, which is related in part to carbon ligand density. Fig. 12 is a plot of α_{PAH} *versus* carbon ligand density for a single silica batch.

Chromatographic characterization of BakerBond Wide-Pore bonded phases, in the form of biopolymer separations, has been described elsewhere for polypeptides [28,29], proteins [30–33] and oligonucleotides [34]. Several are included here to illustrate resolution (Figs. 13 and 14), selectivity (Fig. 15) and speed (Fig. 16).

Fig. 13 is an example of the resolving power of HPLC used in protein sequencing studies. The chromatogram contains peaks corresponding to oxidized peptides from

TABLE 21

VALUES OF SANDER AND WISE SEPARATION (α_{PAH}) FACTOR FOR PRODUCTION BATCHES OF BAKERBOND WIDE-PORE C_{18} 5-μm BONDED PHASE

Lot No.	α_{PAH}	Lot No.	α_{PAH}
085	0.65	484	0.49
145	0.5	129	0.56
154	0.76	131	0.54
143	0.77	116	0.51
160	0.71	101	0.52
917	0.74	097	0.72
487	0.45	113	0.59

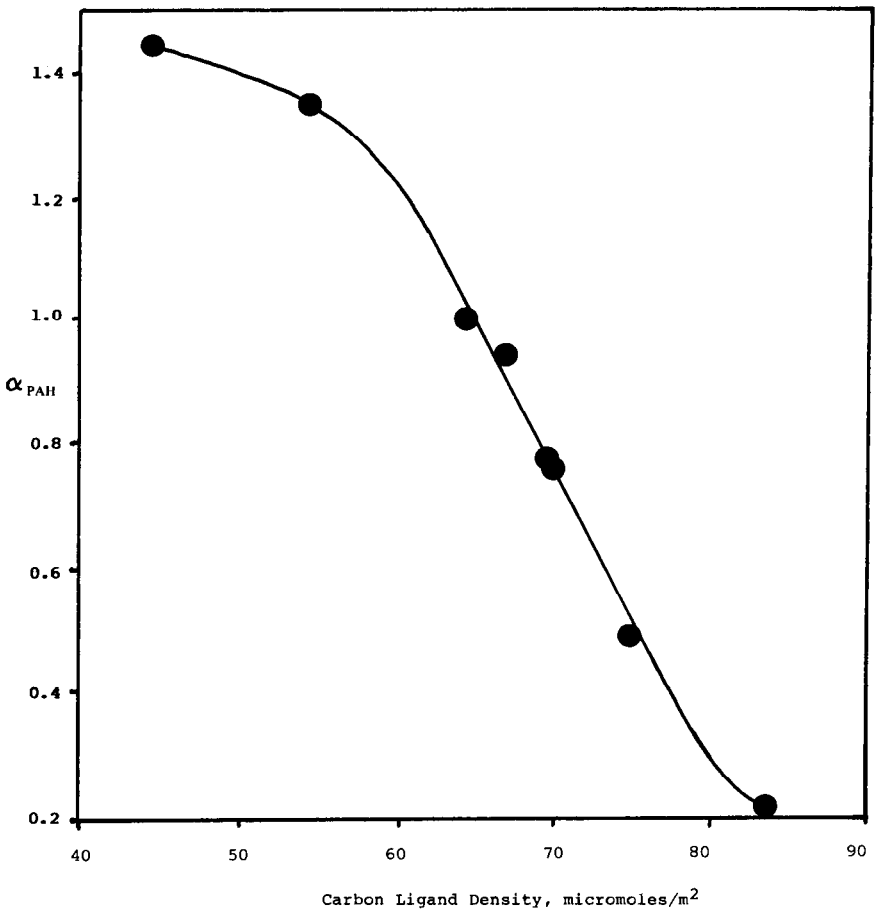

Fig. 12. Relationship between carbon ligand density and the Sander and Wise separation factor, α_{PAH}, for a series of experimental 5-μm C_{18} phases on a 30-nm silica.

the tryptic digest of recombinant bovine somatotropin [35]. The resolving abilities of this technique are such that distinctions can be made between recombinant and pituitary forms of the hormone and the extent of completion of trypsin-catalyzed hydrolysis and the presence of impurities of non-hormonal origin, may be determined.

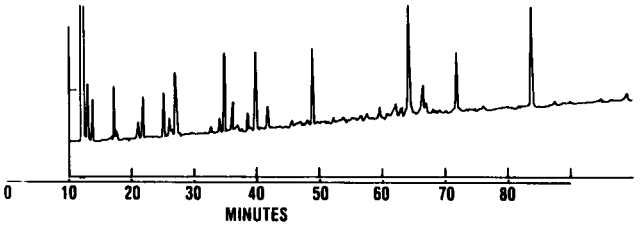

Fig. 13. Reversed-phase chromatography on a BakerBond Wide-Pore C_4, 5-μm column, of the oxidized peptides from the tryptic digest of recombinant bovine somatotropin. See ref. 35 for conditions.

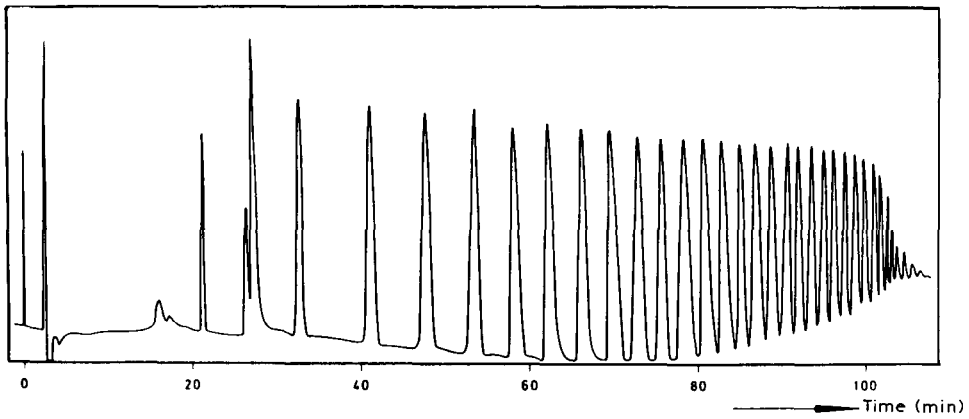

Fig. 14. Anion-exchange chromatography of oligonucleotides from the hydrolysis of poly(rA), on a BakerBond Wide-Pore PEI 5-μm column. See ref. 34 for conditions.

The technique is best applied using wide-pore bonded phases in this example since peaks are sharp and recoveries are high, and peptides from as little as 40 μg of protein may be detected.

Fig. 14 illustrates the ability of our PEI column to resolve oligonucleotides up to

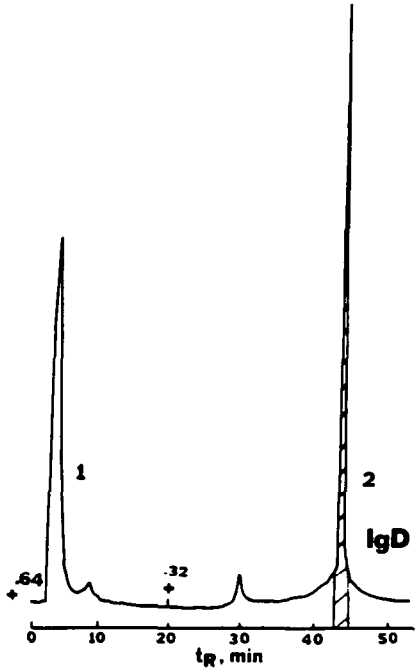

Fig. 15. Separation of an IgD monoclonal antibody from an ascites fluid on BakerBond ABx 5-μm column. Conditions: Column, 250 × 4.6 mm. Buffer A: 10 mM KH_2PO_4, pH 6.0. Buffer B: 250 mM KH_2PO_4, pH 6.8. Gradient: 100% A to 50% A over 60 min. Sample: mouse ascites fluid, 0.5 ml. Peaks: 1 = contains albumins and transferrins from ascites fluid which are not bound to the column; 2 = monoclonal antibody, subclass IgD.

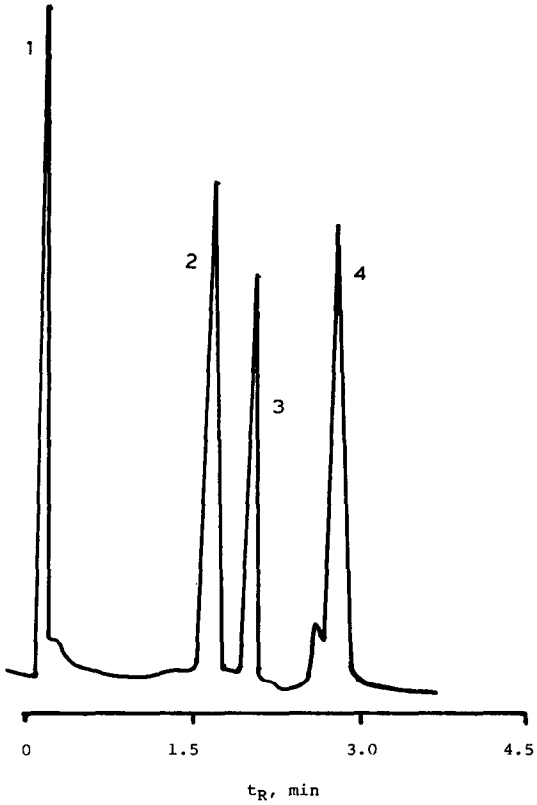

Fig. 16. Rapid separation of four standard proteins by hydrophobic interaction chromatography on a 5-cm BakerBond Wide-Pore HI-Propyl 5-μm column. Conditions: Column 50 × 4.6 mm. Buffer A: 2.0 M $(NH_4)_2SO_4$ plus B. Buffer B: 25 mM KH_2PO_4, pH 7.0. Gradient 100% A to 0% A over 90 s. Flow-rate: 4.0 ml/min. Peaks: 1 = cytochrome c; 2 = myoglobin; 3 = lysozyme; 4 = α-chymotrypsinogen.

chain lengths of 30, from the alkaline hydrolysis of a poly(rA) sample. Capacity is high for these compounds (10 mg per analytical column) and recovery is quantitative [34].

The selectivity of BakerBond ABx for monoclonal antibodies from any source is shown in Fig. 15. This phase was designed to have a maximum affinity for this class of biopolymers, without binding other species such as albumins, transferrins, most proteases, nucleic acids, pyrogens or phenol red. In this example all of these contaminating components elute with the solvent front.

A high speed separation that is achievable with a short column is illustrated in Fig. 16. Although the packing is porous, the temperature is not elevated, and the mobile phase is viscous [due to the presence of 2 M $(NH_4)_2SO_4$], baseline resolution of four proteins is easily achieved in 3 min.

4. APPENDIX 1: DEFINITIONS OF TERMS

Average (or mean): Sum of all values divided by the number of values.

Bonded layer: Organic layer bound to *substrate*.

Bonded phase (also matrix, matrices): A chromatographic stationary phase consisting of a supporting material (such as silica, polystyrene–divinyl benzene co-polymer for example) and an organic layer attached to the support surface by covalent or other bonds.

End-capping: The chemical process of reacting (usually) those silanols that remain after the primary reaction, with a small active silylating reagent (usually trimethylsilyl chloride).

Layer density (LD): See Tables 4 and 5.

Layer thickness (LT): See Tables 4 and 5.

Ligand density (Lig. D): See Tables 4, 5 and 6.

Median: Mid-point of the population.

Mode: Value occurring most frequently.

Pore diameter (PD_s or PD_p, s = substrate, p = bonded phase): See Table 4.

Pore volume (PV_s or PV_p): See Table 4.

Specific layer volume (SLV): See Tables 4 and 5.

Substrate: Supporting material in *bonded phases*.

Surface area (SA_s or SA_p): See Table 4.

5. APPENDIX 2: DERIVATION OF EQUATIONS

Eqn. 2. Carbon Lig. D $= 10^3 \cdot \%C/1.2 \cdot SA$

%C/100 = g C per g bonded phase

Therefore %C/1200 = mol C per g bonded phase

Therefore $\%C/1200 \cdot SA$ = mol C per m^2 bonded phase

or $10^3 \cdot \%C/1.2 \cdot SA$ μmol C per m^2 = carbon Lig. D

Eqn. 3. Lig. D $= 10^3 \cdot \%C/1.2 \cdot$ carbons per ligand $\cdot SA$

$\%C/1200 \cdot$ Carbons per ligand = mol ligand per g

Therefore Lig. D $= 10^3 \cdot \%C/1.2 \cdot$ carbons per ligand $\cdot SA$

Eqn. 4. $SLV = (PV_s - PV_p)\ 10^3/SA$

$PV_s - PV_p$ = Volume of bonded layer in ml/g

Therefore $(PV_s - PV_p)\ 10^3/SA$ = volume of bonded layer per m^2 (mm^3/m^2)

Eqn. 5. $$LD = \frac{\%Organic}{100} \cdot 1/(PV_s - PV_p)$$

%Organic/100 = g bonded layer per g bonded phase

Therefore $\frac{\%Organic}{100} \cdot 1/(PV_s - PV_p)$ = g bonded layer per ml of bonded layer = layer density

Eqn. 6. LT_1 = SLV, expressed in nm.

Let LT = phase thickness in mm

then volume of bonded layer on 1 m^2 in mm^3/m^2

= LT mm $\cdot 10^6$ mm^3/m^2 = SLV

Thus $(LT \cdot 10^6)\ mm^3/m^2$ = (LT in nm) mm^3/m^2 = SLV
Thus LT_1, = SLV, where LT expressed in nm

Eqn. 7. $LT_2 = (PD_s - PD_p)/2$
$PD_s - PD_p$ = difference in pore diameters of substrate, bonded phase
Therefore $PD_s - PD_p/2$ = layer thickness

Eqn. 8. $$v = \frac{n}{4}\frac{(C_p - C_h)}{C_h}$$
Mol ligand per m^2 hydrophilic polymer-clad silica
$= C_h/1200 \cdot$ carbons per ligand $\cdot$ SA
$= C_h/1200 \cdot n \cdot SA$
Increase in %C upon introducing carboxyl groups
$= C_p - C_h$
Therefore moles carbon added $= \frac{C_p - C_h}{1200} \cdot \frac{1}{SA}$ mol C/m^2
Therefore COOH groups added $= \frac{1}{4}\frac{C_p - C_h}{1200} \cdot \frac{1}{SA}$ mol COO/m^2
Therefore mol COOH per mol ligand
$$= \frac{1}{4}(C_p - C_h/1200 \cdot SA)/(C_h/1200\ n \cdot SA)$$
$$= \frac{1}{4}[(C_p - C_h)/(C_h/n)]$$
$$= \frac{n}{4}\frac{(C_p - C_h)}{C_h}$$

Eqn. 9. Lig. D (carboxyl) $= 10^3\ C_h \cdot v/1.2 \cdot n \cdot SA$, μmol/m^2
Mol ligand per m^2 of hydrophilic polymer-clad silica
$= C_h/1200 \cdot n \cdot SA$
Since there are v carboxyl groups per ligand, then mol COOH/m^2
$= v \cdot C_h/1200 \cdot n \cdot SA$
Therefore Lig. D $= 10^3\ C_h \cdot v/1.2 \cdot n \cdot SA$

Eqn. 10. Lig. D $= (C_p - C_h)\ 10^4/48 \cdot SA$
Substituting $v = \frac{n}{4}\frac{(C_p - C_h)}{C_h}$ into eqn. 9:
$$\text{Lig. D} = 10^3 \cdot C_h \cdot \frac{n}{4}\frac{(C_p - C_h)}{C_h}/1.2 \cdot n \cdot SA$$
$$= (C_p - C_h)\ 10^4/48 \cdot SA$$

6. ACKNOWLEDGEMENTS

The data used in this work were generated by a large group of people in our laboratories over several years. In particular I thank Dr. Laura Crane for the stimulating discussions on all aspects of this work and for providing the initial ideas for many of the bonded phase syntheses. Wide-Pore bonded phases were prepared with

great skill by Joseph Mladosich, Michael Jendzeizyk, Donna Baschke, Sunil Kakodkar and Joseph Horvath. Colorimetric analyses were carried out by Shreedhara Murthy, Kathy Silfies and Barbara Barr. HPLC columns were packed by Timothy Krupa, Joseph Cubbage and Michael Schooley. The column titration method was devised by Steve Berkowitz. Elemental analyses and particle size distributions were carried out by Melba Rupell. Mercury porosimetry was the work of Samuel Knochs, Jr. Protein chromatography (Table 18, Figs. 9, 10 and 15) was by Drs. David Nau and Steven Berkowitz (Fig. 16). I thank Bennie Jones for preparing the typescript under adverse conditions.

REFERENCES

1 M. P. Henry, *HPLC in Biotechnology*, Wiley, New York, 1990, Ch. 2, pp. 21–62.
2 K. K. Unger, *Porous Silica, its Properties and Use as Support in Column Liquid Chromatography (J. Chromatogr. Libr.*, Vol. 16), Elsevier, Amsterdam, 1979.
3 S. R. Narayanan, S. Knochs, Jr. and L. J. Crane, *J. Chromatogr.*, 503 (1990) 93.
4 S. Lowell and J. E. Shields, *Powder Surface Area and Porosity*, Chapman & Hall, New York, 1987.
5 T. T. Ngo, *Appl. Biochem. Biotechnol.*, 13 (1986) 207.
6 K. K. Unger, *Packings and Stationary Phases in Chromatographic Techniques*, Marcel Dekker, New York, 1990, pp. 43 and 331.
7 L. C. Sander and S. A. Wise, *Crit. Rev. Anal. Chem.*, 18 (1987) 299.
8 L. R. Snyder and J. J. Kirkland, *Introduction to Modern Liquid Chromatography*, Wiley, New York, 1979, p. 176.
9 Y. Kato, T. Kitamura, A. Mitsui and T. Hashimoto, *J. Chromatogr.*, 398 (1987) 327.
10 D. Johns, *HPLC of Macromolecules*, IRL Press, Oxford, 1989, p. 1.
11 P. T. Matsudaira, *A Practical Guide to Protein and Peptide Purification for Microsequencing*, Academic Press, San Diego, 1989.
12 F. E. Regnier, *High Performance Liquid Chromatography of Proteins and Peptides*, Academic Press, New York, 1983, p. 1.
13 M. T. W. Hearn, *J. Chromatogr.*, 418 (1987) 3.
14 E. Bayer, K. Albert, J. Reiners, M. Nieder and D. Muller, *J. Chromatogr.*, 264 (1983) 197.
15 T. G. Waddell, D. E. Leyden and M. T. DeBello, *J. Am. Chem. Soc.*, 103 (1981) 5303.
16 B. D. Black, E. C. Jennings and J. W. Higgins, presented at the *10th International Symposium on Column Liquid Chromatography, San Francisco, CA, 1986*, paper 509.
17 L. Nendek, B. Buszewski and B. Berek, *J. Chromatogr.*, 360 (1986) 241.
18 R. P. W. Scott and C. F. Simpson, *J. Chromatogr.*, 197 (1980) 11.
19 H. E. Ramsden, *U.S. Pat.*, 4 540 486 (1985).
20 H. E. Ramsden and M. P. Henry, *U.S. Pat.*, 4 551 245 (1985).
21 H. E. Ramsden and D. R. Nau, *U.S. Pat.*, 4 721 573 (1988).
22 L. J. Crane and M. P. Henry, *Protein Recognition of Immobilized Ligands*, A. R. Liss, New York, 1989, p. 59.
23 L. C. Sander and S. A. Wise, *Anal. Chem.*, 62 (1990) 1099.
24 S. A. Berkowitz, *J. Liq. Chromatogr.*, 10 (1987) 2771.
25 L. A. Kennedy, W. Kopaciewicz and F. E. Regnier, *J. Chromatogr.*, 359 (1986) 73.
26 J. J. Kirkland, J. L. Glajch and R. D. Farbe, *Anal. Chem.*, 61 (1989) 2.
27 L. C. Sander and S. A. Wise, *Adv. Chromatogr.*, 25 (1986) 139.
28 P. G. Staunton, B. Grego and M. T. W. Hearn, *J. Chromatogr.*, 296 (1984) 189.
29 D. T. Brandau, P. Ray, A. S. Stern and R. V. Lewis, *Int. J. Peptide Protein Res.*, 25 (1985) 238.
30 S. A. Berkowitz, M. P. Henry, D. R. Nau and L. J. Crane, *Am. Lab.*, 19 (1987) 33.
31 C. Y. Ip and T. Asakura, *Anal. Biochem.*, 156 (1986) 348.
32 A. H. Ross, D. Herlyn and H. Koprowski, *J. Immunol. Meth.*, 102 (1987) 227.
33 D. R. Nau, *Biochromatography*, 1 (1986) 82.
34 A. Pingoud, A. Fliess and V. Pingoud, *HPLC of Macromolecules*, IRL Press, Oxford, 1989, p. 183.
35 P. A. Hartman, J. D. Stodola, G. C. Harbour and J. G. Hoogeheide, *J. Chromatogr.*, 360 (1986) 385.